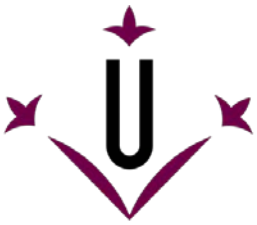

Universitat de Lleida

Carbon isotope discrimination, radial growth, and NDVI share spatiotemporal responses to precipitation in Aleppo pine

Jorge del Castillo, Jordi Voltas, Juan Pedro Ferrio*

Dept. Crop and Forest Sciences-AGROTECNIO Center,

Universitat de Lleida, Rovira Roure 191, E-25198, Lleida, Spain

*Corresponding author, e-mail: pitter.ferrio@pvcf.udl.es

Phone: +34 973 702511

Key message. A common pattern in Aleppo pine $\Delta^{13}C$ responses to both spatial and temporal variability in precipitation was observed, with a general agreement between NDVI, $\Delta^{13}C$ and growth that confirms precipitation as key environmental driver.

Abstract

The aim of this study was to assess the spatio-temporal variability of carbon isotope discrimination ($\Delta^{13}C$) records and its relationship with radial growth (RG) and Normalized Difference Vegetation Index (NDVI) data using a tree-ring network of Aleppo pine (*Pinus halepensis* Mill.) in the eastern part of the Iberian Peninsula. For this purpose, we collected a biennial time series of $\Delta^{13}C$ (1949–1998), together with mean annual precipitation, tree-ring width, and remote sensing (NDVI) data for seven locations along a precipitation gradient. We evaluated how intra-site correlations between variables changed across locations, and how inter-site (or spatial) correlations changed across years. We found that correlations between $\Delta^{13}C$ and precipitation were higher in dry than in wet sites, in agreement with previous studies. Mean RG and NDVI were good indicators of site-specific $\Delta^{13}C$ sensitivity to precipitation. The strongest spatial associations between $\Delta^{13}C$ and precipitation were also found during the driest biennia. However, spatial correlations were strongly affected by carry-over effects of extreme events. Overall, we found a good agreement between $\Delta^{13}C$, NDVI, and RG, although they showed different response patterns to precipitation. We suggest that the combination of these proxies may be useful for monitoring changes in water-use efficiency and productivity at the regional level.

Keywords: carbon isotopes, tree rings, vegetation indices, water-use efficiency, dendroecology

Introduction

Tree rings are extraordinary repositories of climate information. The rising number of tree-ring networks available worldwide can offer new insights on the spatial variability of climate at regional scales (Treydte et al. 2007; Leavitt et al. 2008; del Castillo et al. 2013). Such kind of spatiotemporal information may be relevant to bridge the existing knowledge gap in climate dynamics between large-scale global circulation models and instrumental records of limited geographical coverage (Brayshaw et al., 2011). However, tree sensitivity to climate may vary in time and space for different reasons, including phenotypic plasticity and genetic variability (e.g. Voltas et al. 2008; de Luis et al. 2013), individual life history (Hereş et al. 2012; Voltas et al. 2013), and community structure or local environmental conditions (e.g. Martín-Benito et al. 2011; Moreno-Gutiérrez 2012), among others. Hence, in order to maximise the information retrieved from tree-ring networks, there is a need to explore the environmental drivers underlying spatiotemporal vegetation responses (Treydte et al. 2007; Maseyk et al. 2011; de Luis et al. 2013; del Castillo et al. 2013).

The dendrochronological archive of carbon isotope discrimination ($\Delta^{13}C$) tracks the balance between assimilation rate and stomatal conductance (or intrinsic water-use efficiency; Farquhar and Richards 1984), thus aiding at characterizing tree physiological status (Korol et al. 1999; Ferrio et al. 2003). However, complementary physiological information is needed to disentangle the role of photosynthetic potential, canopy structure and stomatal limitations in determining $\Delta^{13}C$ (Martín-Benito et al. 2011; Moreno-Gutiérrez et al. 2012). In this regard, vegetation indices constitute another type of regional-scale ecological record (Kaufmann 2004; Beck et al. 2013), being now available over a sufficiently long time span as to complement tree-ring records with useful ecophysiological information. In particular, an index of vegetation greenness

such as the Normalized Difference Vegetation Index (NDVI) provides estimates of canopy photosynthetic capacity at different spatial scales through its correlation to both leaf area index (Gamon et al. 1995; Myneni et al. 1997) and the fraction of photosynthetically active radiation absorbed by ecosystems (Gamon et al. 1995).

Previous studies have reported strong positive correlations between summer NDVI and tree-ring width (e.g. Kaufmann 2004; Wang et al. 2004; Beck et al. 2013). Most often summer NDVI appears as the only period of the year related to growth in temperate climates, pointing to the time in which climate exerts the greatest effect on tree-ring width (Kaufmann et al. 2008; Leavitt et al. 2008). However, annual NDVI can be, in some cases, a better integrator of ecosystem productivity, incorporating additional vegetation features such as early spring activity or changes in phenology (Alcaraz-Segura et al. 2008). Thus, the combination of NDVI and tree-ring width, together with climatic data, may offer a better understanding of the biophysical drivers underlying changes in $\Delta^{13}C$ of tree rings.

The main objective of this study was to understand the relationship between climate and tree sensitivity for stable carbon isotopes in *Pinus halepensis* Mill., a widespread, drought-avoidant circum-Mediterranean species, and whether this relationship is subject to variability in time and space. We hypothesised that: 1) the sensitivity of tree-ring $\Delta^{13}C$ to precipitation, as a major biophysical factor modulating ecosystem functioning in Mediterranean climates, would be highly variable in both time and space, hence revealing contrasting tree performances across precipitation gradients; and 2) since NDVI and radial growth are also influenced by precipitation dynamics in drought-prone environments, they must correlate with $\Delta^{13}C$ to a varying degree depending on the particular restrictions imposed by precipitation on tree functioning. To test these

hypotheses, we evaluated the spatio-temporal variability of $\Delta^{13}C$ derived from tree rings of *P. halepensis* and its connection to precipitation, NDVI and tree-ring width records.

Materials and Methods

Study area

The study area is located in the Northeastern Iberian Peninsula, Western Mediterranean basin (Fig. 1). The region is dominated by a Mediterranean climate, with warm and dry summers and mild winters, but also includes continental areas with cool and dry winters, and more humid zones with less seasonality (Table 1). Seven sites were chosen along an annual precipitation gradient ranging from 376 to 835 mm (mean = 562 mm, period 1949–1998; Table 1). Each site was selected to be representative of a distinct eco-geographic region according to the classification of *P. halepensis* provenances (or adaptive units) in Spain (Gil et al. 1996). The provenances represented in this study were: no. 1 (Alta Catalunya; temperate humid Mediterranean); no. 2 (Catalunya Litoral; warm sub-dry Mediterranean maritime); nos. 3, 4, and 5 (Catalunya Interior, Bárdenas-Ribagorza, and Ibérico Aragonés; warm sub-dry sub-Mediterranean); and nos. 6 and 15 (Monegros-Depresión del Ebro and Bética Meridional; warm dry sub-Mediterranean).

Sampling strategy and development of tree-ring chronologies

For each site, we sampled wood cores (5 mm in diameter) at 1.30 m from the south side of 7 to 11 dominant individuals (Table 1). Samples were oven-dried at 60ºC for 48 h and their outermost part removed with a scalpel for tree-ring dating. Tree-ring width was measured with a binocular microscope coupled to a PC with the program TSAP v. 3.0 (Frank Rinn, Heidelberg). We assessed the quality of the chronologies with

COFECHA through calculation of the Expressed Population Signal (*EPS*) statistic (Holmes 1983):

$$EPS = \frac{N \times R}{N \times R + (1 - R)} \quad [1]$$

where N is the number of individuals and R is the mean inter-series correlation. All chronologies reached the threshold of *EPS* = 0.85, ranging from 0.853 in Girona to 0.955 in Lanaja (Table 1).

After cross-dating, standardised ring-width chronologies were built for each site with ARSTAN (Cook and Holmes 1986). First, a double-detrending step was performed for each tree-ring series. The residuals of the first detrending (best-fit curve, linear or exponential) were fitted with a cubic smoothing spline of 50% frequency cut-off of 32 years. This resulted in a standardised tree-ring series for each individual, in the form of:

$$TRW_i = RG_i / F_i \quad [2]$$

where TRW_i, RG_i, and F_i stand for indexed tree-ring width, measured ring width (or radial growth), and fitted ring width, respectively, at year i. Subsequently, each series was modelled as a stationary autoregressive process, resulting in a 'residual' index chronology. Finally, a composite autoregressive model across all tree-ring series was added to each 'residual' chronology, resulting in the 'arstan' chronology (Cook and Holmes 1986). All subsequent analyses were performed using 'arstan' chronologies.

Carbon isotope discrimination in tree rings

For stable isotope analysis, we pooled samples across individual trees and every 2 years (from 1949–1950 to 1997–1998) at each site. This decision stemmed from the need to balance the recovery of high-frequency variability in the isotopic signal against analytical cost. For the sake of comparison, we checked the loss in annual variability of

143 TRW_i associated with a hypothetical biennial analysis of tree-ring series, which ranged
144 from 23.4% in Rasquera to 40.0% in Lanaja (mean = 33.1%). This indicates that
145 approximately two-thirds of the original TRW_i signal had been retained if using this
146 pooling procedure.
147 After pooling, samples were milled (IKA-A10) to a fine powder. To minimize juvenile
148 effects, we omitted the first 20 years of cambial age (Loader et al. 2010). We used intact
149 wood tissue for carbon isotope analyses (i.e., without any chemical pre-treatment) since
150 whole wood provides more consistent relationships with climatic variables for this
151 species compared with particular wood fractions (e.g., holocellulose; Ferrio and Voltas
152 2005). The $^{13}C/^{12}C$ ratios of wood samples were determined by mass spectrometry and
153 the results expressed as isotopic composition ($\delta^{13}C$) relative to the international standard
154 Vienna PeeDee Belemnite (VPDB).
155 To take into account temporal changes in the isotope composition of atmospheric CO_2
156 ($\delta^{13}C_{atm}$), carbon isotope discrimination ($\Delta^{13}C$) was calculated (Farquhar and Richards
157 1984):
158 $$\Delta^{13}C = (\delta^{13}C_{atm} - \delta^{13}C_{plant}) / (1 + \delta^{13}C_{plant}) \quad [3]$$
159 $\delta^{13}C_{atm}$ was inferred by interpolating data from two Antarctic stations (Halley Bay and
160 Palmer Station) of the CU-INSTAAR/NOAA-CMDL network for atmospheric CO_2
161 measurements, as described in Ferrio et al. (2005). Estimated $\delta^{13}C_{atm}$ for the time period
162 represented in each sample ranged from -6.9 to -7.9‰.

163 *Meteorological data*

164 Monthly values of temperature and precipitation for the study period (1949–1998) were
165 obtained from the Instituto Nacional de Meteorología and the Confederación
166 Hidrográfica del Ebro. Wherever the altitude of the sampling site exceeded that of the

meteorological station, we applied a 0.6ºC decrease in temperature every 100 m and a 8% precipitation increment per 100 m, except for July and August, when precipitation is mostly convective and not related to altitude (Gandullo 1994). A seasonality index (SI) was calculated following Walsh and Lawler (1981):

$$SI_i = \frac{1}{R_i} \sum_{n=1}^{n=12} \left| X_{in} - \frac{R_i}{12} \right| \qquad [4]$$

where R_i is the total annual precipitation for year i and X_{in} is the monthly precipitation for month n. According to this index, sites with SI = 0.60–0.79 are classified as 'seasonal', whereas those with SI = 0.80–0.99 are classified as 'markedly seasonal with a long dry season'.

Remote sensing data

Time series of NDVI were obtained from the Global Inventory Modeling and Mapping Studies (GIMMS) dataset covering the period 1982–1998 at a biweekly temporal resolution (University of Maryland, 2004; available at http://glcf.umd.edu/data/gimms/). The NDVI data has a 9 × 9 km spatial resolution, and we collected a single pixel representative of each forest stand of our study sites. To compensate for the limited spatial resolution, we selected the pixels in order to maximize the fractional area covered by forest stands, and checked the seasonal variation of the index to confirm that the temporal spectra was typical of conifer forests. Biweekly NDVI data were recalculated as annual and seasonal mean NDVI for further temporal analysis (January to March = winter; April to June = spring; July to September = summer; October to December = autumn). For the analysis of spatial signals in tree-ring width and $\Delta^{13}C$, we used the site mean NDVI for the period 1982–1998.

190

191 *Data analysis*

192 Annually (for RG and NDVI) or biennially resolved (for $\Delta^{13}C$) data were subjected to
193 analysis of variance, with site and time included as factors in the model. Relationships
194 between climate and physiological variables were assessed using simple Pearson
195 correlations (*r*), either across the annual (or biennial, when involving $\Delta^{13}C$) chronology
196 for each site or across long-term means of all sites (hereafter, intra-site and inter-site
197 analyses, respectively). We then related the *r* values of the relationship between $\Delta^{13}C$
198 and precipitation at the site level to the site means and coefficients of variation (CVs) of
199 precipitation, $\Delta^{13}C$, and NDVI. This was done to identify possible factors underlying the
200 varying strength of this relationship. By definition, mean values of tree-ring width
201 indices (TRW_i) fall around unity at all sites; thus, for inter-site analyses we used mean
202 values of RG for the period 1949–1998 obtained as the average of the median growth of
203 each tree to minimize the effect of extreme years. On the other hand, we used indexed
204 values (TRW_i) in all calculations involving temporal variability in radial growth (i.e.,
205 intra-site correlations and inter-annual coefficients of variation) to avoid artifacts due to
206 age trends.

207

208 **Results**

209 *Variability and relationships between tree growth, $\Delta^{13}C$ and NDVI*

210 Radial growth (RG) varied significantly among sites from 0.8 ±0.19 mm (Riba-roja) to
211 2.1 ±0.35 mm (Girona), with a mean of 1.1 ±0.17 mm. Besides, there were significant
212 differences in $\Delta^{13}C$ among sites, ranging from 15.6 ±0.12 ‰ in Riba-roja to 17.3 ±0.11
213 ‰ in El Grado, with a mean value of 16.6 ±0.28 ‰. Intra-site correlations (*N*=25)

between indexed tree-ring widths (TRW_i) and $\Delta^{13}C$ values were positive and significant for three (out of seven) sites (Purchena, Riba-roja and Rasquera), whereas a marginally significant ($p = 0.07$) positive correlation was found between RG and $\Delta^{13}C$ at the spatial (i.e., inter-site) level (Table 2).

Annual NDVI values varied significantly among sites from 0.34 ±0.082 (Purchena) to 0.63 ±0.045 (Girona), with a mean of 0.44 ±0.040. We found positive temporal (i.e., intra-site) associations between biennial $\Delta^{13}C$ and NDVI (N=9), but they were significant only at three sites (Rasquera, El Grado and Girona) (Table 2). Similarly, we found a significant positive inter-site correlation between mean annual NDVI and long-term mean $\Delta^{13}C$ (Table 2). Intra-site correlations between annual NDVI and TRW_i (N=17) were positive and significant at two sites (Purchena and Riba-roja), and a significant positive correlation was also observed across sites between mean annual NDVI and mean RG (Table 2).

Generally TRW_i showed stronger correlations with summer NDVI (correlation coefficients, r, ranging from 0.35 in Valderrobres to 0.84 in Riba-roja) than with annual or other seasonal NDVI, except for Girona and Lanaja, which exhibited negligible correlations with summer NDVI (r = 0.02 for Girona; r = 0.05 for Lanaja). Correlations between $\Delta^{13}C$ and summer NDVI were stronger than with other NDVI values at three of the driest sites (r = 0.61, 0.62 and 0.74 in Riba-roja, Lanaja and Rasquera, respectively), weaker at the wettest sites (r = 0.40 and 0.70 for El Grado and Girona, respectively), and similar in Purchena and Valderrobres.

Climate factors determining tree growth, $\Delta^{13}C$, and NDVI

Overall, RG was positively related to annual precipitation both at the temporal (intra-site, using TRW_i, N=50) and spatial (inter-site, using mean RG, N=7) levels (Table 2). Nevertheless, temporal correlations were only significant at four sites. Precipitation seasonality was significantly correlated with TRW_i only at the driest site (Purchena) (Table 2). Temperature usually showed slightly weaker correlations with TRW_i than precipitation, being negatively related to TRW_i at four sites but positively correlated at the wettest site (Girona) (Table 2). RG did not show significant temperature dependence at the spatial level.

We found strong positive correlations between precipitation and $\Delta^{13}C$ at five sites (biennial records, N=25), but this relationship was not significant at the wettest sites (El Grado and Girona) (Table 2). Precipitation also showed a strong positive inter-site correlation with $\Delta^{13}C$ (r = 0.90; P < 0.01). In contrast, no significant correlations were found between temperature and $\Delta^{13}C$, and SI was significantly and negatively correlated with $\Delta^{13}C$ only at the two extremes of the precipitation gradient (Purchena and Girona) (Table 2).

We only found a significant intra-site correlation between annual NDVI and precipitation at Riba-roja (N=17, Table 2). In contrast, NDVI showed a strong positive inter-site correlation with precipitation. For temperature, we only found a significant negative correlation with annual NDVI at one site (Valderrobres), while SI showed a strong negative correlation with annual NDVI at both extremes of the precipitation gradient (Purchena and Girona) (Table 2). Annual precipitation showed higher correlations with summer NDVI than with other seasonal NDVI values at all sites, except in Lanaja and Girona. Nevertheless, correlations with summer NDVI were only significant at the two driest sites (r = 0.49 and r = 0.57 in Purchena and Riba-roja,

261 respectively). However, annual NDVI showed tighter correlations with temperature and
262 SI than seasonal NDVI values.
263
264 *General trends in the response of $\Delta^{13}C$ to precipitation across sites*
265 The best precipitation model accounting for $\Delta^{13}C$ variability involved a log fitting to the
266 complete dataset (r^2 = 0.59, N = 175, P < 0.001;~~,~~ Fig. 2). Still, a linear model fitted
267 equally well $\Delta^{13}C$ records if values above 800 mm were not considered (r^2 = 0.60, N =
268 155, P < 0.001;~~,~~ Fig. 2). A similar result was observed for the relationship between
269 long-term site means of $\Delta^{13}C$ and annual precipitation (period 1949–1998), which was
270 best explained using a log model (r^2 = 0.89, N = 7, P < 0.01, not shown).
271
272 *Site-dependent temporal responses of $\Delta^{13}C$ to precipitation*
273 A number of potential variables underlying the temporal sensitivity of $\Delta^{13}C$ to
274 precipitation were investigated by correlation analysis. We found a significant negative
275 correlation between r values of $\Delta^{13}C$ *vs*. precipitation (N = 25) and mean site
276 precipitation (Fig. 3a). However, the relationship between r values of $\Delta^{13}C$ *vs*.
277 precipitation and CVs of precipitation (instead of mean site values) was not significant
278 (Fig. 3b). Conversely, a significant positive association was found between r values of
279 $\Delta^{13}C$ *vs*. precipitation and CVs of $\Delta^{13}C$ (Figs. 3c, d), whereas the relationship involving
280 $\Delta^{13}C$ mean records was not significant. There was a strong negative association between
281 site r values and RG means, but no significant trend with CV of TRW_i (Figs. 3e, f). We
282 also observed a significant negative correlation with site means of annual NDVI, and a
283 positive correlation with CV of annual NDVI (Figs. 3g, h). We did not find any

significant correlation with mean or CV values of either temperature or SI (results not shown).

Time-dependent spatial responses of $\Delta^{13}C$ to precipitation

In order to explore whether the observed long-term spatial relationship between $\Delta^{13}C$ and precipitation was consistent over time, this relationship was evaluated for 25 biennia independently for the period 1949–1998. Only a marginally significant ($P < 0.10$) negative trend was detected with both mean precipitation and mean $\Delta^{13}C$ (results not shown). Two clear outliers, corresponding to the biennia 1985–1986 and 1987–1988, were detected, which presented rather low *r* values (Fig. 4, crosses). For both biennia, we found that precipitation in the precedent biennium 1983–1984 (the driest in the period 1949–1998) was better linked to $\Delta^{13}C$ than the precipitation of the actual years (Fig. 4, triangles). By excluding these outliers, both mean precipitation and mean $\Delta^{13}C$ showed significant negative correlations with *r* values of $\Delta^{13}C$ *vs*. precipitation ($r = -0.51$ and $r = -0.45$, respectively). We did not find significant correlations with the remaining variables.

Discussion

Site-specific responses of $\Delta^{13}C$ to precipitation

By combining biennial data from seven sites we observed a saturation point of $\Delta^{13}C$ around 800 mm, above which $\Delta^{13}C$ was hardly sensitive to annual precipitation. The log function describing the relationship between both variables is almost identical to that reported for *P. halepensis* by Ferrio et al. (2003) using a 25-year tree-ring pool ($\Delta^{13}C = 4.6 + 1.9 \times \ln(P)$; $r^2 = 0.59$; $P < 0.001$). In line with this overall trend, our results also

indicate that the association between $\Delta^{13}C$ and precipitation is stronger at sites where the mean annual precipitation is lower and weaker where it is higher (Fig. 3a). A lower sensitivity of $\Delta^{13}C$ to precipitation as water availability increases has been reported for *P. halepensis* (Klein et al. 2005; Maseyk et al. 2011) and other conifers (e.g. Korol et al. 1999; Warren et al. 2001). When water becomes less limiting, site-specific factors such as soil properties (Korol et al. 1999; Treydte et al. 2007) or stand attributes (e.g., canopy height or density) (Fernandez et al. 2007; Moreno-Gutiérrez et al. 2012) tend to blur the relationship between $\Delta^{13}C$ and precipitation. These factors may also affect the $\Delta^{13}C$ signal in drier sites; however, under such conditions precipitation is still the most limiting factor for tree performance, at least for drought-avoidant species such as *P. halepensis* (Ferrio et al. 2003; Ferrio & Voltas 2005; Del Castillo et al. 2013). Additionally, $\Delta^{13}C$ can be also affected by the yearly pattern of rainfall distribution (see e.g. Korol et al. 1999). In this regard, the negative correlation between SI and $\Delta^{13}C$ at the wettest site suggests that precipitation distribution may have a stronger effect than total annual precipitation under near-optimal conditions.

Is the spatial response of $\Delta^{13}C$ to precipitation consistent over time?

The analysis of the spatial relationship between $\Delta^{13}C$ and precipitation for 2-year periods pointed to tighter associations in dry than in wetter biennia (Fig. 4a). However, spatial responses showed erratic variations through time. Different physiological processes may obscure the spatial dependence of $\Delta^{13}C$ on precipitation, with an expected stronger effect over short time periods than for long-term site-specific signals. For instance, year to year carry-over effects may imprint a significant isotopic signature lasting for 2 or more years (see e.g., Sarris et al. 2013). After particularly extreme years, $\Delta^{13}C$ of subsequent years may correlate well with the environmental conditions of the

event year. In this regard, we observed exceptional carry-over effects in the biennia 1985–1986 and 1987–1988 (Fig. 4), in which the spatial $\Delta^{13}C$ variation was better explained by the precipitation occurring in the biennium 1983–1984 (the driest of the entire record). Alternatively, water stress can lead to limited carbon loading in the phloem, as well as to readjustments of leaf area, reducing wood production and causing an uncoupling of leaf and tree-ring signals (Cernusak et al. 2013; Voltas et al. 2013).

Cross-links between physiological responses and tree growth

NDVI was highly correlated with precipitation across sites (Table 2, r = 0.94), in agreement with previous studies reconstructing spatial patterns of precipitation from annual NDVI in the Iberian Peninsula (Immerzeel et al. 2009). At the temporal level, summer NDVI correlated better with $\Delta^{13}C$ at three drought-prone sites, whereas correlations with annual NDVI were stronger for the two wettest sites. Overall, these relationships were weaker than that obtained across sites, although these results are not conclusive due to the limited number of records and the loss of temporal variability due to tree-ring pooling (N=9 and N=7, for temporal and spatial correlations, respectively).

Correlations between TRW_i and either NDVI or $\Delta^{13}C$ were generally stronger at drier sites. Tree productivity, in terms of radial growth, seed or foliage production, has already been linked to growing season-integrated NDVI in oak trees (Wang et al. 2004). This explains the observed link to annual NDVI in *P. halepensis*, which can grow all year around if conditions are favourable. In this regard, tree-ring growth can be strongly limited by water availability in Mediterranean environments, which explains the tight correlation with both $\Delta^{13}C$ and summer NDVI at dry sites. The negative correlation between TRW_i and temperature at four sites can be interpreted as a response to increasing evaporative demand (Ferrio and Voltas 2005; de Luis et al. 2013; Maseyk et

al. 2011). On the contrary, a positive correlation with temperature at the wettest site (Girona) agrees with previous observations reporting on growth limitations associated with winter cold (de Luis et al. 2013). Hence, where $\Delta^{13}C$ is responsive to variations in precipitation, $\Delta^{13}C$, TRW_i, and summer NDVI share a strong common signal. In contrast, the link between $\Delta^{13}C$ and annual NDVI, as a surrogate of productivity, tends to be stronger at the wettest environments.

Remote sensing and carbon isotopes as complementary proxies for water-use efficiency

An interesting outcome of this study is that NDVI correlated well with both $\Delta^{13}C$ and TRW at the spatial level, with a number of significant relationships also emerging at the temporal level. Given the strong spatial agreement between NDVI and $\Delta^{13}C$, the combination of tree-ring $\Delta^{13}C$ networks (*isoscapes*, see, e.g., Leavitt et al. 2008; del Castillo et al. 2013) and high-resolution NDVI data may allow to spatially model historical stand attributes, including productivity or water-use efficiency (Leavitt et al. 2008; Beck et al. 2013). Furthermore, NDVI appears as a good proxy for site-specific sensitivity of $\Delta^{13}C$ to precipitation, and could be used to pre-select potentially sensitive tree-ring sampling sites for paleoenvironmental research. Nevertheless, we still could observe site-specific deviations in NDVI not reflected in precipitation and $\Delta^{13}C$ (Fig. 3, Fig. 5). Besides potential differences in stand attributes affecting NDVI, Aleppo pine is a thermophilous species with polycyclic growth (see e.g. de Luis et al. 2013) that, due to extended phenology, may produce comparatively denser canopies in warm (Riba-roja) than in cold (El Grado) sites, but having little effect on $\Delta^{13}C$ (Figs. 3 and 5). Additionally, NDVI tends to increase at a faster rate than $\Delta^{13}C$ (Fig. 5), more likely due to changes in leaf area rather than changes in leaf chlorophyll content, since the latter

would have an opposite effect on $\Delta^{13}C$: leaves with higher photosynthetic activity would show higher water-use efficiency and, thus, lower $\Delta^{13}C$ (Farquhar and Richards 1984; Cernusak et al. 2013). Still, both chlorophyll content and leaf area tend to decrease under drought conditions in *P. halepensis* (Baquedano and Castillo 2006) and, thus, NDVI might hold a signal from both variables, particularly in drought-prone environments (Pasquato 2013). Hence, the poor agreement between $\Delta^{13}C$ and NDVI at the temporal scale in the driest sites could be the result of a greater relevance of the chlorophyll content signal controlling NDVI in water-limited environments.

Conclusions

Our results confirm precipitation as a key driver of variations in tree growth, water-use efficiency, and vegetation greenness for Aleppo pine. We observed a broad common pattern in the response of $\Delta^{13}C$ to both spatial and temporal variability in precipitation, showing a saturation response of $\Delta^{13}C$ when water becomes less limiting. In this regard, inter-site differences in the sensitivity of $\Delta^{13}C$ to precipitation are mainly linked to the frequency of water-limiting conditions in the time series. The general agreement between NDVI, $\Delta^{13}C$ and tree growth opens the possibility to integrate information from tree-ring networks and satellite data to monitor changes in water-use efficiency and productivity at regional scales.

Conflict of interest

The authors declare that they have no conflicts of interest.

Author contributions

406 Study idea by J.P.F.; all authors designed the research, analysed the data, interpreted the
407 results and wrote the paper.
408

References

Alcaraz-Segura D, Cabello J, Paruelo J (2008) Baseline characterization of major Iberian vegetation types based on the NDVI dynamics. Plant Ecol 202:13–29

Baquedano FJ, Castillo FJ (2006) Comparative ecophysiological effects of drought on seedlings of the Mediterranean water-saver *Pinus halepensis* and water-spenders *Quercus coccifera* and *Quercus ilex*. Trees 20:689–700

Beck PSA, Andreu-Hayles L, D'Arrigo R et al (2013) A large-scale coherent signal of canopy status in maximum latewood density of tree rings at arctic treeline in North America. Glob Planet Change 100:109–118

Brayshaw, D. J., C. M. C. Rambeau and S. J. Smith (2011), Changes in Mediterranean climate during the Holocene: Insights from global and regional climate modelling, The Holocene, 21(1), 15-31

Cernusak LA, Ubierna N, Winter K, Holtum JA, Marshall JD, Farquhar GD (2013) Environmental and physiological determinants of carbon isotope discrimination in terrestrial plants. New Phytol 200:950–965

Cook ER, Holmes RL (1986) User manual for program ARSTAN. In: Holmes RL, Adams RK, Fritts HC (eds) Tree-ring chronologies of Western North America: California, eastern Oregon and northern Great Basin. Laboratory of Tree-Ring Research, University of Arizona, pp 50–65

de Luis M, Cufar K, I Filippo A, Ovak K, Apadopoulos A, Iovesan G, Athgeber CB, Aventós J, Az MA, Mith KT (2013) Plasticity in dendroclimatic response across the distribution range of Aleppo pine (*Pinus halepensis*). PLoS ONE 8:e83550

del Castillo J, Aguilera M, Voltas J, Ferrio JP (2013) Isoscapes of tree-ring carbon-13 perform like meteorological networks in predicting regional precipitation patterns. J Geophys Res Biogeosci 118: 352-360.

Farquhar GD, Richards RA (1984) Isotopic composition of plant carbon correlates with water-use efficiency of wheat genotypes. Aust J Plant Physiol 11:539–552

Fernandez I, González-Prieto SJ, Cabaneiro A (2007) 13C-isotopic fingerprint of *Pinus pinaster Ait.* and *Pinus sylvestris* L. wood related to the quality of standing tree mass in forests from NW Spain. Rapid Commun Mass Spectrom 19:3199–3206

Ferrio JP, Araus JL, Buxó R, Voltas J, Bort J (2005) Water management practices and climate in ancient agriculture: inference from the stable isotope composition of archaeobotanical remains. Vegetation History and Archaeobotany 14:510–517

Ferrio JP, Florit A, Vega A et al (2003) $\Delta^{13}C$ and tree-ring width reflect different drought responses in *Quercus ilex* and *Pinus halepensis*. Oecologia 137:512–518

457 Ferrio JP, Voltas J (2005) Carbon and oxygen isotope ratios in wood constituents of
458 *Pinus halepensis* as indicators of precipitation, temperature and vapour pressure
459 deficit. Tellus B 57B:164–173
460
461 Gamon JA, Field CB, Goulden ML et al (1995) Relationships between NDVI,
462 canopy structure, and photosynthesis in three Californian vegetation types. Ecol
463 Appl 5:28–41
464
465 Gandullo JM (1994) Climatología y ciencia del suelo. Fundación Conde del Valle
466 de Salazar, Madrid
467
468 Gil L, Díaz-Fernández PM, Jiménez P, Roldán M, Alía R, Agúndez D, DeMiguel J,
469 Martín S, DeTuero M (1996) Las Regiones de procedencia de *Pinus halepensis*
470 *Mill*. en España. O.A. Parques Nacionales, Madrid.
471
472 Hereş AM, Martínez-Vilalta J, López BC (2012) Growth patterns in relation to
473 drought-induced mortality at two Scots pine (*Pinus sylvestris* L.) sites in NE Iberian
474 Peninsula. Trees – Structure and Function 26:621–630
475
476 Holmes RL (1983) Computer-assisted quality control in tree-ring dating and
477 measurement. Tree-Ring Bull. 43: 69-78
478
479 Immerzeel WW, Rutten MM, Droogers P (2009) Spatial downscaling of TRMM
480 precipitation using vegetative response on the Iberian Peninsula. Remote Sens
481 Environ 113:362–370

Kaufmann RK, D'Arrigo RD, Laskowski C, Myneni RB, Zhou L, Davi NK (2004) The effect of growing season and summer greenness on northern forests. Geophys Res Lett 31:L09205

Kaufmann RK, D'Arrigo RD, Paletta LF et al (2008) Identifying climatic controls on ring width: the timing of correlations between tree rings and NDVI. Earth Interact 12:1–14

Klein T, Hemming D, Lin T, Grünzweig JM, Maseyk K, Rotenberg E, Yakir D (2005) Association between tree-ring and needle $\delta^{13}C$ and leaf gas exchange in *Pinus halepensis* under semi-arid conditions. Oecologia 144: 45-54

Korol RL, Kirschbaum MUF, Farquhar GD, Jeffreys M (1999) Effects of water status and soil fertility on the C-isotope signature in *Pinus radiata*. Tree Physiol 19:551–562

Leavitt SW, Chase TN, Rajagopalan B et al (2008) Southwestern U.S. tree-ring carbon isotope indices as a possible proxy for reconstruction of greenness of vegetation. Geophys Res Lett 35:L12704

Loader NJ, Helle G, Los SO, Lehmkuhl F, Schleser GH (2010) Twentieth-century summer temperature variability in the southern Altai Mountains: a carbon and oxygen isotope study of tree-rings. Holocene 20: 1149–1156

Martín-Benito D, Kint V, del Río M, Muys B, Cañellas I (2011) Growth responses of West-Mediterranean *Pinus nigra* to climate change are modulated by competition and productivity: Past trends and future perspectives. Forest Ecology and Management 262:1030–1040

Maseyk K, Hemming D, Angert A, Leavitt SW, Yakir D (2011) Increase in water-use efficiency and underlying processes in pine forests across a precipitation gradient in the dry Mediterranean region over the past 30 years. Oecologia 167:573–585

Moreno-Gutiérrez C, Battipaglia G, Cherubini P, Saurer M, Nicolás E, Contreras S, Querejeta JI (2012) Stand structure modulates the long-term vulnerability of *Pinus halepensis* to climatic drought in a semiarid Mediterranean ecosystem. Plant Cell Environ 35:1026–1039

Myneni RB, Ramakrishna R, Nemani R, Running SW (1997) Estimation of global leaf area index and absorbed par using radiative transfer models. IEEE Trans Geosci Remote Sens

Pasquato M (2013) Comparison of parsimonious dynamic vegetation modelling approaches for semiarid climates, PhD Thesis. University of Valencia

Sarris D, Siegwolf R, Körner C (2013) Inter- and intra-annual stable carbon and oxygen isotope signals in response to drought in Mediterranean pines. Agric For Meteorol 168:59–68

Soil Survey Staff (2010) 'Keys to Soil Taxonomy, 11th ed.' (USDA-Natural Resources Conservation Service: Washington,D.C.)

Treydte K, Frank D, Esper J et al. (2007) Signal strength and climate calibration of a European tree-ring isotope network. Geophys Res Lett 34 L24302

Voltas J, Camarero JJ, Carulla D, Aguilera M, Ortiz A, Ferrio JP (2013) A retrospective, dual-isotope approach reveals individual predispositions to winter-drought induced tree dieback in the southernmost distribution limit of Scots pine. Plant Cell Environ 36:1435–1448

Voltas J, Chambel MR, Prada MA, Ferrio JP (2008) Climate-related variability in carbon and oxygen stable isotopes among populations of *Aleppo pine* grown in common-garden tests. Trees-Structure and Function 22:759–769

Walsh PD, Lawler DM (1981) Rainfall seasonality: description, spatial patterns and change through time. Weather 36:201–208

Wang J, Rich PM, Price KP, Kettle WD (2004) Relations between NDVI and tree productivity in the central Great Plains. Int J Remote Sens 25:3127–3138

Warren C, McGrath J, Adams M (2001) Water availability and carbon isotope discrimination in conifers. Oecologia 127:476–486

557 **Figure captions**

558 **Fig. 1** Map of the study area and sampling sites, depicting mean annual precipitation
559 according to the Digital Climatic Atlas of the Iberian Peninsula
560 (http://www.opengis.uab.es/wms/iberia/mms/index.htm). Numbers correspond to
561 provenance regions as indicated in Table 1.

562

563 **Fig. 2** Scatterplot depicting linear (below 800 mm precipitation) and log relationships
564 between annual precipitation and carbon isotope discrimination ($\Delta^{13}C$) (biennial
565 records; period 1949-1998) at seven sampling sites. Dotted vertical line indicates the
566 approximate threshold for a linear response.

567

568 **Fig. 3** Intra-site correlation coefficients (*r*) of the relationship between time-series of
569 annual precipitation and carbon isotope discrimination ($\Delta^{13}C$) (biennial records; period
570 1949-1998, *N*=25) as a function of: a) long-term mean annual precipitation; b) inter-
571 annual coefficient of variation (CV) of precipitation; c) long-term mean $\Delta^{13}C$; d) inter-
572 biennial CV of $\Delta^{13}C$; e) mean annual NDVI (1982–1998); f) inter-annual CV of NDVI;
573 g) long-term mean of radial growth (RG); and h) inter-annual CV of tree-ring width
574 indices (TRW_i). Dashed lines indicate the threshold value for significance ($P < 0.05$).

575

576 **Fig. 4** Inter-site correlation coefficients (*r*) of the relationship between annual
577 precipitation and carbon isotope discrimination ($\Delta^{13}C$) (biennial records; period 1949-
578 1998, *N*=7) and: a) mean annual precipitation for each biennium; b) inter-site coefficient
579 of variation (CV) of mean annual precipitation; c) biennial $\Delta^{13}C$; and d) inter-site CV of

580 $\Delta^{13}C$. Dashed lines indicate the threshold value for significance ($P < 0.05$). Crosses
581 indicate outliers showing weak correlations with current precipitation (biennia 1985-
582 1986 and 1987-1988), but better correlated with precipitation during the driest biennium
583 (1983-1984, correlations shown with open triangles). See text for details.

584 **Fig. 5** Regression plots illustrating the log relationship between Normalized Difference
585 Vegetation Index (NDVI) and carbon isotope discrimination ($\Delta^{13}C$) across seven
586 sampling sites at a biennial scale (period 1949–1998): a) annual NDVI; and b) summer
587 NDVI. The arrow indicates the increasing precipitation gradient among study sites.

588

589

590 **Table 1.** Main eco-geographic and climatic characteristics of the seven sites included in

591 this work, together with the chronology statistics.

Site description					Climate			Soil Group	Chronology		
Prov.	**Site**	**Latitude**	**Longitude**	**Alt. (m)**	**P (mm)**	**T (ºC)**	**SI**		***N***	**EPS**	**Period**
1	Girona	42º01'	03º00'E	190	835	14.0	0.66	Haploxerept	8	0.85	1948-1999
2	Rasquera	41º01'	00º36'E	180	547	15.3	0.82	Xerorthent	8	0.93	1926-1999
3	Riba-roja	41º20'	00º30'E	80	395	15.1	0.73	Torriorthent	11	0.95	1936-1999
4	El Grado	42º09'	00º15'E	625	652	12.6	0.60	Haploxerept	8	0.94	1928-2000
5	Valderrobres	40º53'	00º12'E	630	648	13.9	0.77	Haploxeralf	10	0.94	1938-1999
6	Lanaja	41º50'	00º32'W	380	469	13.1	0.74	Xerorthent	11	0.96	1884-1999
15	Purchena	37º26'	02º20'W	900	376	16.6	0.81	Torriorthent	7	0.93	1919-1999

592 Prov., provenance region, following Gil et al. (1996); Alt., altitude; P, mean annual precipitation; T, mean
593 annual temperature. SI, seasonality index, according to Walsh and Lawler (1981); *N*, number of trees;
594 EPS, expressed population signal. Soil groups according to USDA Soil Taxonomy (Soil Survey Staff
595 2010).
596

Table 2. Pearson correlation coefficients between physiological parameters (carbon isotope discrimination [$\Delta^{13}C$], indexed tree-ring width [TRW_i], and mean annual Normalized Difference Vegetation Index [NDVI]) involving annual or biennial (for correlations with $\Delta^{13}C$) records (period 1949–1998) at the site level (upper section). Pearson correlation coefficients between physiological parameters ($\Delta^{13}C$, TRW_i, and NDVI) and climatic records of annual precipitation (P), mean annual temperature (T), and precipitation seasonality index (SI) at the site level (lower section). *N*, number of common observations. The last column shows inter-site correlations of long-term means (1949–1998, $N = 7$) involving the same variables, except for tree-ring width, in which original values of radial growth (RG) were used instead of TRW_i. $*P < 0.05$; $*P < 0.01$; $***P < 0.001$.

Variables	*N*	Purchena	Riba-roja	Lanaja	Rasquera	Valderrobres	El Grado	Girona	Inter-site
TRW_i vs $\Delta^{13}C$	25	**0.61****	**0.58****	0.36	**0.42***	0.27	-0.04	0.03	0.67
NDVI vs $\Delta^{13}C$	9	0.44	0.52	0.42	**0.70***	-0.03	**0.81****	**0.81****	**0.75 ***
NDVI vs TRW_i	17	**0.58***	**0.69****	0.21	0.27	0.19	0.42	-0.16	**0.91****
P vs TRW_i	50	**0.61*****	**0.39****	**0.36***	0.09	0.07	**0.42****	0.23	**0.91****
T vs TRW_i	50[1]	**-0.37***	0.03	**-0.30***	**-0.33***	-0.08	**-0.36****	**0.30***	-0.34
SI vs TRW_i	50	**-0.33***	-0.16	-0.21	-0.14	0.22	0.02	-0.06	-0.62
P vs $\Delta^{13}C$	25	**0.68*****	**0.64*****	**0.61****	**0.58****	**0.67*****	0.34	0.07	**0.90****
T vs $\Delta^{13}C$	25[1]	0.11	0.29	-0.24	0.18	0.28	-0.04	0.33	-0.67
SI vs $\Delta^{13}C$	25	**-0.55****	-0.15	-0.16	0.05	0.04	-0.20	**-0.44***	-0.52
P vs NDVI	17	0.35	**0.51***	-0.17	-0.02	0.16	0.05	-0.07	**0.94****
T vs NDVI	17	0.37	0.40	0.24	-0.12	**-0.60***	0.10	0.33	-0.41
SI vs NDVI	17	**-0.61****	-0.20	0.07	0.03	-0.11	0.13	**-0.62****	-0.56

[1]For Purchena, due to missing temperature data, $N = 41$ years (for TRW_i) and $N = 21$ biennia (for $\Delta^{13}C$).

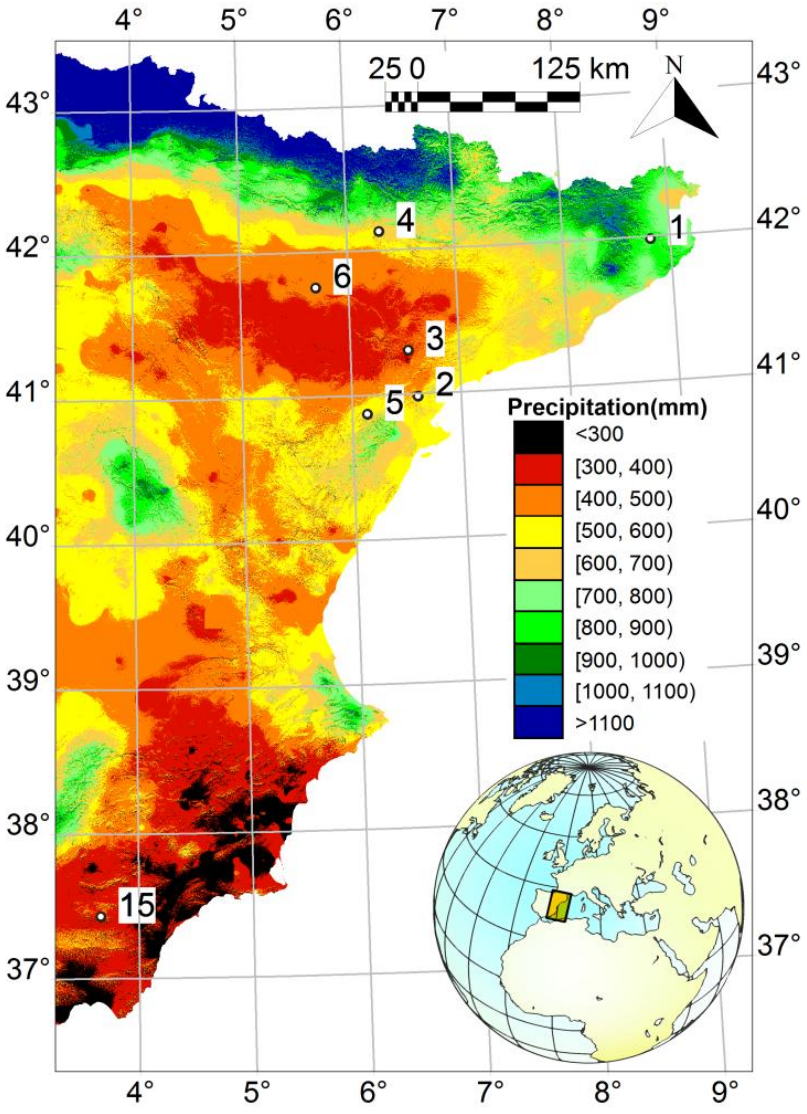

611

612

613

614 Fig. 1

615

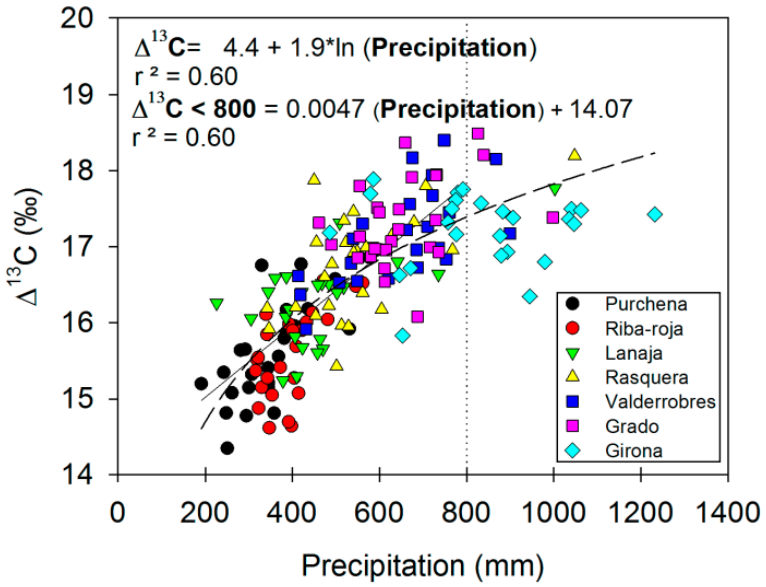
Δ13C= 4.4 + 1.9*ln (Precipitation)
r ² = 0.60
Δ13C < 800 = 0.0047 (Precipitation) + 14.07
r ² = 0.60
Δ13C (‰)
Precipitation (mm)
Purchena
Riba-roja
Lanaja
Rasquera
Valderrobres
Grado
Girona

Fig. 2

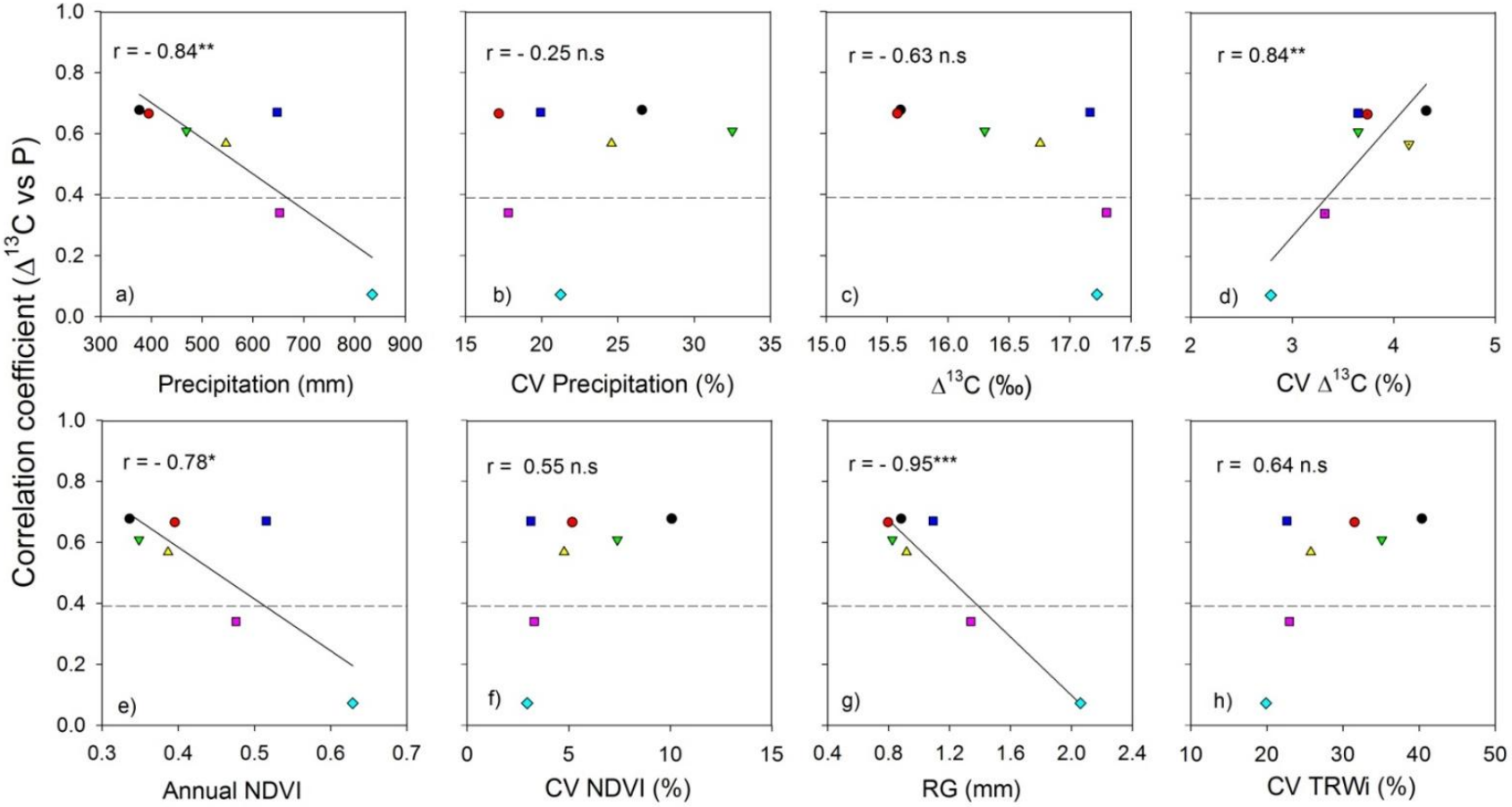
Correlation coefficient (Δ13C vs P)
r = - 0.84**
a)
Precipitation (mm)
r = - 0.25 n.s
b)
CV Precipitation (%)
r = - 0.63 n.s
c)
Δ13C (‰)
r = 0.84**
d)
CV Δ13C (%)
r = - 0.78*
e)
Annual NDVI
r = 0.55 n.s
f)
CV NDVI (%)
r = - 0.95***
g)
RG (mm)
r = 0.64 n.s
h)
CV TRWi (%)

Fig. 3

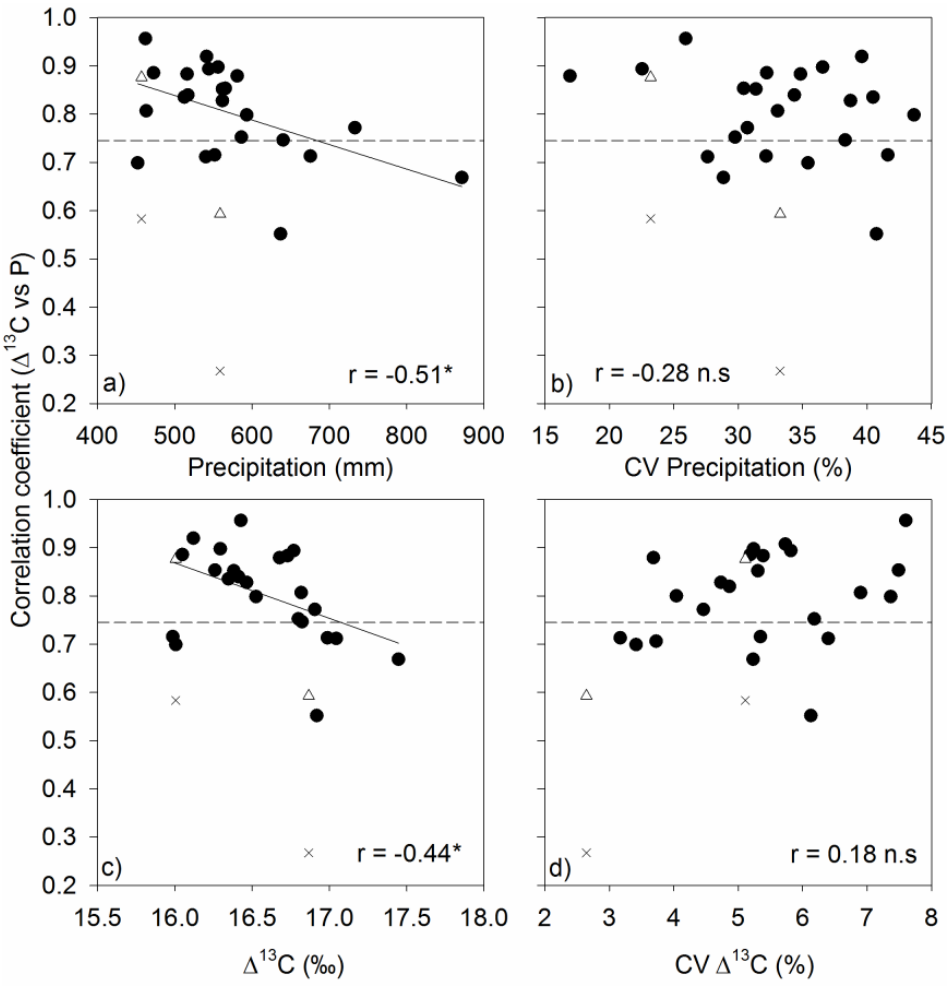
Correlation coefficient (Δ13C vs P)
a)
r = -0.51*
Precipitation (mm)
b)
r = -0.28 n.s
CV Precipitation (%)
c)
r = -0.44*
Δ13C (‰)
d)
r = 0.18 n.s
CV Δ13C (%)

Fig. 4

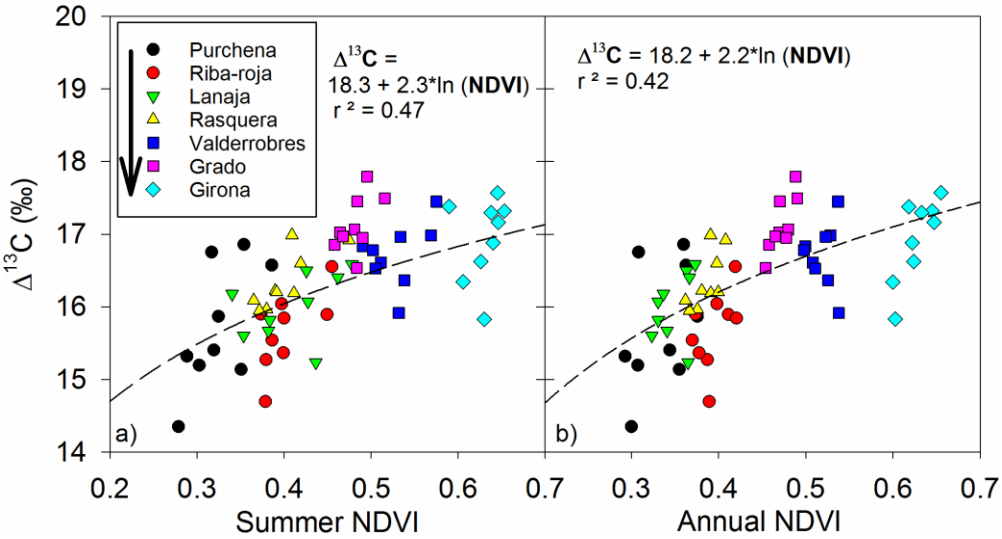
Purchena
Riba-roja
Lanaja
Rasquera
Valderrobres
Grado
Girona
Δ13C =
18.3 + 2.3*ln (NDVI)
r ² = 0.47
Δ13C = 18.2 + 2.2*ln (NDVI)
r ² = 0.42
Δ13C (‰)
a)
b)
Summer NDVI
Annual NDVI

Fig. 5